Positively selected FimH residues enhance virulence during urinary tract infection by altering FimH conformation

Drew J. Schwartz[a], Vasilios Kalas[a], Jerome S. Pinkner[a], Swaine L. Chen[b,c], Caitlin N. Spaulding[a], Karen W. Dodson[a], and Scott J. Hultgren[a,1]

[a]Center for Women's Infectious Disease Research, Department of Molecular Microbiology, Washington University School of Medicine, St. Louis, MO 63110; and [b]Division of Infectious Diseases, Department of Medicine, Yong Loo Lin School of Medicine, National University of Singapore, Singapore 119074; and [c]Infectious Diseases Group, Genome Institute of Singapore, Singapore 138672

This contribution is part of the special series of Inaugural Articles by members of the National Academy of Sciences elected in 2011.

Contributed by Scott J. Hultgren, August 12, 2013 (sent for review July 14, 2013)

Chaperone–usher pathway pili are a widespread family of extracellular, Gram-negative bacterial fibers with important roles in bacterial pathogenesis. Type 1 pili are important virulence factors in uropathogenic *Escherichia coli* (UPEC), which cause the majority of urinary tract infections (UTI). FimH, the type 1 adhesin, binds mannosylated glycoproteins on the surface of human and murine bladder cells, facilitating bacterial colonization, invasion, and formation of biofilm-like intracellular bacterial communities. The mannose-binding pocket of FimH is invariant among UPEC. We discovered that pathoadaptive alleles of FimH with variant residues outside the binding pocket affect FimH-mediated acute and chronic pathogenesis of two commonly studied UPEC strains, UTI89 and CFT073. In vitro binding studies revealed that, whereas all pathoadaptive variants tested displayed the same high affinity for mannose when bound by the chaperone FimC, affinities varied when FimH was incorporated into pilus tip-like, FimCGH complexes. Structural studies have shown that FimH adopts an elongated conformation when complexed with FimC, but, when incorporated into the pilus tip, FimH can adopt a compact conformation. We hypothesize that the propensity of FimH to adopt the elongated conformation in the tip corresponds to its mannose binding affinity. Interestingly, FimH variants, which maintain a high-affinity conformation in the FimCGH tip-like structure, were attenuated during chronic bladder infection, implying that FimH's ability to switch between conformations is important in pathogenesis. Our studies argue that positively selected residues modulate fitness during UTI by affecting FimH conformation and function, providing an example of evolutionary tuning of structural dynamics impacting in vivo survival.

protein conformations | microbial pathogenesis | chronic cystitis | protein dynamics

Urinary tract infections (UTIs) are common infections causing serious morbidity and significant expenditures in healthcare dollars and lost wages. Women are disproportionately affected, with over half of women experiencing at least one UTI during their lifetime (1). In the absence of treatment, 50–80% of women will resolve a UTI within 2 mo, but up to 60% of women may remain bacteriuric with or without symptoms for at least 5–7 wk after the initial infection (2). Furthermore, even when effective therapy is given and bacteriuria and symptoms of the acute UTI resolve, 25–40% of women experience a recurrent UTI (rUTI) (2, 3). rUTI can occur by recolonization of the urinary tract from the gastrointestinal (GI) tract or from another environmental source by the same or different strain or may be due to reactivation of the original UTI strain from a bladder reservoir (4–6). Uropathogenic *Escherichia coli* (UPEC) cause 80–90% of community-acquired UTI and 50% of nosocomial UTI (7). The increasing prevalence of multidrug-resistant organisms can prolong the infection (8). Thus, chronic and recurrent UTI represents a major health concern worldwide, necessitating molecular understanding of disease pathogenesis and investigations into novel diagnostics and therapies.

UTI is a highly complex disease involving colonization of multiple niches, each of which presents a unique set of evolutionary pressures shaping host–microbe and microbe–microbe interactions involving a multitude of virulence factors that determine disease onset, progression, and outcome. Adhesive pili assembled by the chaperone–usher pathway (CUP), such as type 1 pili, are well-characterized UPEC UTI virulence determinants. Type 1 pili, like other CUP pili, contain an adhesin (FimH) at their tip that plays an important role in host–pathogen interactions and biofilm formation. Type 1 pili are nearly ubiquitous among clinical UPEC isolates (9, 10) as well as commensal *E. coli* and other *Enterobacteriaceae*. Expression of type 1 pili is essential for colonization of the murine urinary tract (11); however, expressing type 1 pili is not sufficient for long-term colonization, as commensal *E. coli* are rapidly cleared (12).

Upon UPEC entrance into the bladder, FimH binds mannosylated glycoproteins, including uroplakins expressed throughout human and murine bladders (13). Subsequent to attachment, UPEC invade superficial facet cells in a FimH-dependent manner (12, 14) and replicate in the cytoplasm, forming large biofilm-like structures called intracellular bacterial communities (IBCs) (15).

Significance

The evolution of multidrug resistance in pathogenic bacteria, including uropathogenic *Escherichia coli* (UPEC), that cause most urinary tract infections is becoming a worldwide crisis. UPEC use a variety of virulence factors and adhesins, including the mannose-binding FimH adhesin, to colonize and invade bladder tissue, often forming intracellular biofilms and quiescent reservoirs that can contribute to recurrent infections recalcitrant to treatment. Using two prototypical UPEC strains, we discovered that positively selected residues outside of the FimH mannose-binding pocket affect transitions between low- and high-affinity FimH conformations, which extraordinarily impacts FimH function during pathogenesis. Thus, this work elucidates mechanistic and functional insights into pathoadaptation and evolutionary fine-tuning of critical virulence interactions.

Author contributions: D.J.S., V.K., S.L.C., and S.J.H. designed research; D.J.S., V.K., J.S.P., S.L.C., and C.N.S. performed research; V.K. and J.S.P. contributed new reagents/analytic tools; D.J.S., V.K., and S.J.H. analyzed data; and D.J.S., S.L.C., K.W.D., and S.J.H. wrote the paper.

The authors declare no conflict of interest.

Freely available online through the PNAS open access option.

See Profile on page 15509.

[1]To whom correspondence should be addressed. E-mail: hultgren@borcim.wustl.edu.

This article contains supporting information online at www.pnas.org/lookup/suppl/doi:10.1073/pnas.1315203110/-/DCSupplemental.

The formation of IBCs has been observed for numerous clinical UPEC isolates in multiple mouse models and in exfoliated uroepithelial cells in urines of patients with acute UTI, but not from healthy controls (16, 17). The process of invasion and IBC formation provides UPEC an ability to survive stringent bottlenecks during pathogenesis in the urinary tract (18, 19). Outcomes of infection range from resolution with or without accompanying quiescent intracellular reservoirs (QIRs) in the bladder tissue (4) to persistent bacteriuria and chronic cystitis (20). In C3H/HeN mice, the formation of a high number of IBCs at 6 h postinfection (hpi) and an exuberant systemic innate immune response at 24 hpi, measurable in both urine and serum, correlate with the development of chronic cystitis marked by persistent urine and bladder titers $>10^4$ cfu/mL and severe bladder immunopathology (18, 20). In addition to colonizing the bladder, UPEC can ascend the ureters and infect the kidneys, leading to pyelonephritis. The connection between acute and chronic UTI is just now beginning to be characterized (21–23).

Type 1 pili and the tip adhesin, FimH, are encoded by the *fim* operon (24, 25). Mature FimH is a 279-aa two-domain protein containing a mannose-binding lectin domain (residues 1–150) and a pilin domain (residues 159–279) with an 8-aa linker connecting the domains (Fig. 1) (26–28). The mannose-binding pocket of FimH is invariant among sequenced UPEC (26, 29); however, several residues outside the mannose-binding pocket (positions 27, 62, 66, and 163) were found to be evolving under positive selection in clinical UPEC isolates compared with fecal strains (Fig. 1) (29, 30, 31). Among four fully sequenced UPEC isolates (UTI89, CFT073, 536, and J96), differences exist in positively selected residues 27, 62, and 163 (Table 1). Clinical isolates expressing different *fimH* alleles have observable differences in the degree of pathogenicity as measured by IBC formation (16) and the development of chronic cystitis (20). We found that UTI89, a cystitis isolate, formed more IBCs and had higher bladder titers at 6 hpi than CFT073, a pyelonephritis isolate, in single infections and coinfections. Because of the demonstrated importance of type 1 pilus function in pathogenesis, we conducted *fimH* allele swap experiments to determine whether the differences in *fimH* between UPEC strains were responsible for the phenotypic differences. We generated CFT073 and UTI89 strains containing different *fimH* alleles inserted into the normal chromosomal position. We found that presence of a *fimH* sequence encoding FimH from UTI89 (denoted FimH::A62/V163) resulted in significant increases in IBC development and the propensity to cause chronic cystitis compared with expression of CFT073 FimH (FimH::S62/A163). In coinfections, strains expressing FimH::A62/V163 significantly outcompeted otherwise isogenic strains harboring FimH::S62/A163 in both CFT073 and UTI89. FimH complexed with its chaperone FimC adopts an elongated conformation (Fig. 1*A*), which binds mannose with high affinity (26, 37). When complexed with the FimG adaptor, FimH can adopt a compact conformation that binds mannose with low affinity (Fig. 1*B*) (37). The identity of residues at positively selected positions outside the binding pocket dramatically impacts the mannose binding affinity of FimH when in the FimCGH tip-like complex but not in the FimCH complex. Thus, we argue that the combination of residues at positively selected positions affects the propensity of FimH to adopt an elongated conformation in the tip and thus its relative mannose binding affinity. FimH alleles that retained the high-affinity binding conformation in the tip were significantly attenuated in a mouse model of UTI, suggesting that equilibrium between FimH conformations, which is modulated by positively selected residues, is critical in pathogenesis.

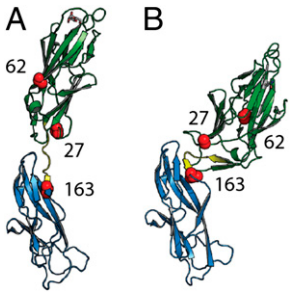

Fig. 1. FimH positively selected residues. FimH is a two-domain adhesin comprised of a lectin domain of residues 1–150 (green), a pilin domain with residues 159–279 (blue), and a linker loop (yellow) connecting them. Positively selected residues are mapped onto the structures of FimH as red spheres. (*A*) In the elongated FimH (V27/S62/V163) structure, mannose is observed at the distal binding pocket in white sticks (J96 FimH; PDB ID code: 1KLF; FimC removed for clarity). (*B*) In the compressed FimH (A27/S62/A163) structure in the absence of mannose, position 133 of the binding pocket is colored white (F18 FimH; PDB ID code: 3JWN). Note the distance of these positively selected residues from the mannose binding pocket.

Results

Prevalence of Positively Selected FimH Alleles in Humans. Comparing UPEC-infected urine isolates to fecal *E. coli* from healthy humans and animals has previously identified genes and residues within genes under positive selection in UPEC (29, 38, 39). We analyzed a collection of *fimH* sequences obtained from 33 fecal *E. coli* from healthy, uninfected humans as well as 232 urine and periurethral isolates from women suffering acute or rUTI, asymptomatic bacteriuria, or pyelonephritis (16, 17, 29, 40–43). We were particularly interested in cataloguing naturally occurring residue combinations at positions 27, 62, and 163 because, in previous studies, these residues showed evidence of positive selection, and mutations in these residues impacted fitness of the cystitis isolate UTI89 (29). In sequences of fecal *E. coli* and *E. coli* from infected urine, we found one of two residues at each of these positions. An alanine occurred at position 27 in 85% of fecal isolates and 81% of urine isolates whereas a valine occurred at position 27 in the other sequenced isolates. A serine occurred at position 62 in all of the fecal isolates and in 93% of urine isolates whereas an alanine occurred in 7% of urine isolates. At position 163, a valine occurred in all fecal isolates and in 93% of urine isolates, with alanine occurring in the other 7% of urine isolates. Of the eight possible combinations of these three residues, we found only the four combinations shown in Table 1. Most *E. coli* isolates encode FimH::A27/S62/V163, with this allele being present in a higher percentage of fecal strains than urine strains. The prototypical UPEC isolates UTI89 and CFT073 encode two different pathoadaptive FimH variants, A27/A62/V163 and A27/S62/A163, respectively. Neither *fimH* allele was observed in healthy feces (Table 1). All other residues in the mature FimH of UTI89 and CFT073 are identical. UTI89 was isolated from the urine of a patient experiencing an uncomplicated acute UTI (12). CFT073 was isolated from the blood and urine of a woman suffering acute pyelonephritis and sepsis (44). Because of these differences in occurrence of different *fimH* alleles in different types of clinical samples, we examined their impact on pathogenesis in the urinary tract.

FimH Sequence Modulates IBC Number. We first performed a systematic analysis of the differences in infection between UTI89 and CFT073. We transurethrally inoculated female C3H/HeN mice with 10^7 or 10^8 cfu of UTI89 or CFT073 in 50 μL of PBS (Fig. 2). The median number of IBCs formed at 6 hpi was significantly higher for UTI89 than the number of IBCs formed by CFT073 at both inoculum concentrations (Fig. 2*A*). Similar, statistically significant results were observed at 6 hpi in whole-bladder titers (Fig. 2*B*). Bacterial titers at 6 hpi in the kidneys (Fig. 2*C*) did not significantly differ between strains, and we observed only a slight increase in kidney titers with an increased UTI89 inoculum.

To assess the impact of different *fimH* alleles in isogenic UTI89 and CFT073 backgrounds, we conducted *fimH* allele swaps. Hereafter, we will refer to these FimH alleles by the residue expressed at the relevant, positively selected position. We examined the effect on pathogenesis of three *fimH* alleles in each

Table 1. Prevalence of positively selected FimH residues

Residue*	Frequency in healthy feces† (%)	Frequency in urine/periurethra† (%)	Sequenced analog‡
V27/S62/V163	5/33 (15)	49/254 (19)	MG1655/J96
A27/A62/V163	0	19/254 (7)	UTI89/NU14
A27/S62/A163	0	17/254 (7)	CFT073/536
A27/S62/V163	28/33 (85)	169/254 (67)	None

*All other possibilities not observed.
†The 287 strains used from human *Eschericia coli* collection of reference (ECOR) (40) and clinical *E. coli* isolates with 33 fecal samples from uninfected women and 254 infected urine/periurethral isolates.
‡Published strain for which *fimH* sequence is available (32–36, 38). No fully sequenced analog of A27/S62/V163 is published.

background: A62/V163, S62/V163, and S62/A163. Except for the previously published in vitro defects of FimH::S62/V163 (29), we saw no effect of FimH variants on growth in LB media in single and coculture (Figs. S1*A* and S2), status of the *fim* promoter (Fig. S1*B*), total surface piliation (Fig. S1*C*), or 1 hpi invasion into 5637 cultured bladder cells (Fig. S1*D*) in either the UTI89 or CFT073 backgrounds. We found a moderate, but statistically significant, twofold increase in guinea pig red blood cell hemagglutination (HA) for FimH::A62/V163 in both strain backgrounds (Fig. S1*E*) and 48 h biofilm formation in LB in PVC plates in CFT073 (Fig. S1*F*). A reproducible HA titer difference of twofold has previously been shown to affect IBC formation (29). Accordingly, we saw that CFT073 encoding FimH::A62/V163 (UTI89 FimH) resulted in a greater number of IBCs (Fig. 3*A*) than WT CFT073 in an independent challenge experiment. No statistically significant difference in 6 hpi IBC number was obtained between UTI89 FimH::A62/V163 and UTI89 FimH::S62/A163, suggesting possible strain-dependent effects. Additionally, it is possible that subtle *fim* regulation defects exist in vivo even though we observed no differences in vitro with these strains.

FimH Sequence Modifies Ability to Persist During Chronic Cystitis. We then assessed the effect of FimH variation on development of chronic cystitis. Sixty-eight percent of mice developed persistent bacteriuria and chronic cystitis with bladder titers greater than 10^4 cfu at sacrifice 4 wk postinfection (wpi) when infected with 10^7 cfu UTI89 expressing its cognate FimH::A62/V163 compared with 40% of mice infected with UTI89 expressing the CFT073 cognate allele FimH::S62/A163 ($P < 0.05$; Fig. 3*B*). CFT073, expressing its cognate FimH::S62/A163 caused chronic cystitis in only 23% of mice, statistically significantly different from both UTI89 FimH::A62/V163 (**68**%) ($P < 0.0005$) and CFT073 FimH::A62/V163 (**47**%) ($P < 0.05$; Fig. 3*B*). Kidney titers were also increased for both UTI89 and CFT073 strains expressing FimH::A62/V163 (Fig. 3*C*), which likely reflects the higher bladder titers and the noted vesicoureteral reflux and/or ability of UPEC to ascend the ureters in this model (18, 45).

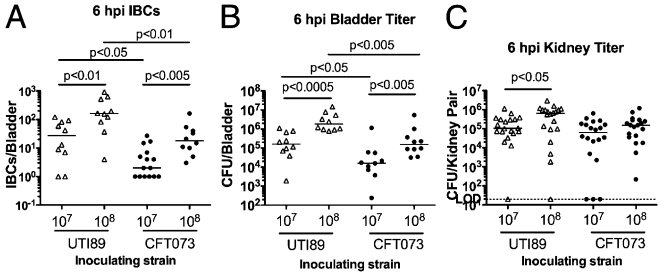

Fig. 2. CFT073 and UTI89 acutely infect mouse urinary tracts. (*A*) IBCs per bladder were enumerated with LacZ stain. (*B*) Total bladder bacterial counts were determined after homogenization. (*C*) Total bacteria present in both kidneys were enumerated. $n = 2$ experiments with five mice per group. *C* includes kidney titers of mice from *A* and *B*.

Strains Expressing FimH::A62/V163 Displace Strains Expressing FimH::S62/A163 During Chronic Coinfection. We found that, in both backgrounds, strains expressing FimH::A62/V163 had subtle, yet significant, increases in tissue occupation versus strains expressing FimH::S62/A163 after coinfections (Fig. S3). At 3 hpi, 1.7- to 1.8-fold more bacteria encoding FimH::A62/V163 were found in the gentamicin-protected fraction in both strain backgrounds (Fig. S3). At 6 hpi, 2.2-fold more cfu of CFT073 FimH::A62/V163 was obtained (Fig. S3*B*). In addition to this acute advantage, strains expressing FimH::A62/V163 outcompeted strains expressing FimH::S62/A163 in the bladders and kidneys of mice experiencing chronic cystitis at 4 wpi based on $\log_{10}$ competitive index in both strain backgrounds (Fig. 4; $P < 0.005$, Wilcoxon Signed Rank). With the average chronic cystitis bladder containing 10^7 cfu at 4 wk, a $\log_{10}$CI of >5 indicates that strains with FimH::S62/A163 are near the limit of detection (20 cfu). The median $\log_{10}$ CI for coinfecting UTI89 FimH::A62/V163 $Spect^R$ and UTI89 FimH::S62/A163 Kan^R was also significantly higher than a control competition between UTI89 Kan^R and UTI89 $Spect^R$ with the same *fimH*, confirming that the difference in antibiotic resistance marker could not account for the infection phenotypes (Fig. S4). Thus, in coinfections, independent of strain background, expressing FimH::A62/V163 was advantageous over expressing FimH::S62/A163 in the urine as well as in chronic organs at four wpi (Fig. 4).

UTI89 Outcompetes CFT073 in Coinfection Experiments even When Expressing the Same FimH. To further clarify the relative contribution of FimH differences versus other factors in UTI89 and CFT073 for different pathogenic phenotypes, we conducted additional coinfection experiments. We first coinoculated CFT073 and UTI89 each expressing their natural *fimH* allele. UTI89 had higher titers than CFT073 in the bladder lumen as well as the intracellular compartment (Fig. S5 *A*, *B*, and *D*). We observed no difference between UTI89 and CFT073 in the kidneys (Fig. S5*C*). We then coinoculated UTI89 and CFT073, both of which were expressing FimH::A62/V163, and found that UTI89 outcompeted CFT073 during chronic cystitis even when both expressed the same *fimH* allele (Fig. 4*C*), suggesting that UTI89 expresses other factors that, in addition to its *fimH* allele, contribute to chronic cystitis.

Positively Selected FimH Residues Impact Affinity, but Only When FimH Is Incorporated into a Tip-Like Complex. We hypothesized that the fitness advantage of expressing FimH::A62/V163 over FimH::S62/A163 throughout infection was due to differences in the ability to bind mannosylated epitopes on the bladder surface. Therefore, we used BioLayer Interferometry to assess mannose binding of different FimH variants. FimH is known to adopt two different conformations that vary in their affinity for mannose (37): an elongated conformation with high mannose affinity and a compressed conformation with low mannose affinity (Fig. 1). In the first set of binding experiments, FimCH complexes were used in which FimC traps FimH in the elongated, high mannose binding conformation (37, 46). We immobilized biotinylated BSA-mannose on SuperStreptavidin pins and tested for binding of FimCH complexes in solution. For these assays, we used FimH

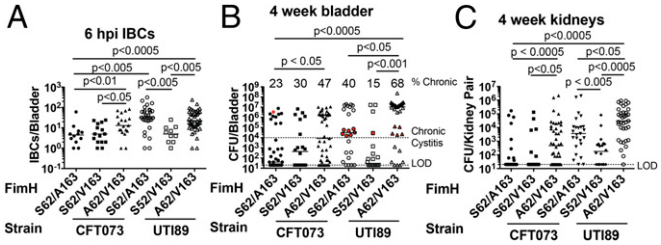

Fig. 3. FimH allele modulates acute and chronic pathogenesis. Mice were infected with 10^7 cfu (range 3.4×10^6 to 1.8×10^7; median 1.02×10^7) of the indicated strains. (*A*) IBCs were enumerated after LacZ staining. (*B*) Urine was collected at days 1, 7, 14, and 21, and the number of bacteria present in bladders was determined at 4 wpi. Data points above 10^4 cfu reflect mice that had persistent bacteriuria and are considered to have chronic cystitis. Red symbols denote mice that resolved bacteriuria and either had a recurrence or high levels of reservoir titers, and were thus included in the resolved category because they did not experience chronic cystitis. The percentage of mice experiencing chronic cystitis is displayed at the top of each column. (*C*) Kidney titers of the mice from *B*. (*A*) $n = 2$–11 experiments with two to eight mice per group. (*B* and *C*) $n = 2$–8 experiments with 5–10 mice each.

with variations at positions 62 and 163 as seen in UTI89 and CFT073. We also varied position 27 because this position was previously found to be under positive selection (29); this residue is variable in both uropathogens and fecal strains (Table 1). All FimCH complexes had very similar affinity to BSA-mannose regardless of the variant with the exception of FimH::Q133K, which has a mutation within the mannose binding pocket resulting in an inability to bind to mannose (Fig. 5*A*) (26). The FimCH fit curves had very high R^2 values and K_D values between 1.5 and 4.2 μM (Table 2), consistent with previously reported affinity calculations for the isolated FimH lectin domain (46).

Each variant was then reconstituted into a tip-like $FimC_{his}GH$ complex in vitro by combining $FimC_{his}G$ and FimCH (Fig. 5*B*). In addition to $FimC_{his}GH$ complexes, small quantities of higher-order structures such as $FimC_{his}GGH$ and $FimC_{his}GGGH$ were detected, but the distributions of these complexes were equal among *fimH* alleles. FimH within the $FimC_{his}GH$ complex is able to adopt the compact conformation seen in tip structures, as the lectin domain is no longer restrained from bending by FimC (37, 47, 48). In the tip-like $FimC_{his}GH$ complexes, different FimH alleles elicited dramatic differences in BSA-mannose binding affinity (Fig. 5*C*), with three general affinity patterns: high, intermediate, and low. $FimC_{his}GH$::V27/A62/A163 and $FimC_{his}GH$::A27/A62/A163 maintained the same high affinity as their FimCH counterparts (Table 2, Fig. 5), suggesting that these variants may not adopt the compressed, low-affinity conformation in the pilus or that their propensity to transition to the elongated state is increased, accounting for higher relative affinities. The UTI89 natural variant (FimH::A27/A62/V163) and CFT073 natural variant (FimH::A27/S62/A163) both showed intermediate affinity when in the $FimC_{his}GH$ complexes. However, $FimC_{his}GH$::A27/A62/V163 had a significant ($P = 0.0087$, Mann–Whitney *U* Test), twofold higher affinity than $FimC_{his}GH$::A27/S62/A163 (1.2 vs. 2.5×10^{-4} M; Table 2). A twofold difference in FimH K_D would likely translate to a very large difference in adherence in piliated UPEC containing 20–200 pili per bacterium (Fig. S1*C*). $FimC_{his}GH$::A27/S62/V163 and $FimC_{his}GH$::Q133K both had low affinity, with K_D values in the 3 mM range (Table 2). This observation suggests that FimH::A27/S62/V163 may not be able to adopt the elongated high-affinity conformation as efficiently.

To assess whether higher binding correlated with increased infection, we coinfected mice with UTI89 expressing either of the high-affinity FimH variants, FimH::A27/A62/A163 or FimH::V27/A62/A163 and WT UTI89 (Fig. 5*D*). Both FimH::A27/A62/A163 and FimH::V27/A62/A163, but not the WT control, were attenuated in the bladders of mice 4 wpi compared with WT UTI89 (Table 2). This result suggests that mannose-binding affinity does not directly correlate with pathogenicity. Instead, an intermediate binding affinity is the best predictor of virulence, implying that FimH may dynamically interconvert between conformations depending on the local environment.

Discussion

The looming worldwide crisis of globally spreading, multidrug-resistant microorganisms (49), the growing body of work delineating the important benefits of the host's normal microbiota (50), and the deleterious effects of broad-spectrum antimicrobial treatments on these symbiotic/commensal relationships (51) argue that we need to develop new approaches to treat and prevent common infectious diseases such as UTI. With the delineation of Koch's postulates and Falkow's molecular postulates (52, 53), infectious-disease experts have learned to associate a particular disease with the presence or absence of a particular pathogen or "virulence factor," respectively, in a diseased host. In considering UTI pathogenesis, a critical factor is that virulence is not simply dichotomous (presence/absence of a microorganism in the host or virulence factor within a bacterium). Outcomes of infectious disease in general, and UTIs specifically, are determined by a complex, yet seemingly subtle, interplay between differing host genetics and immune states (54, 55), host experiences/exposures (56, 57), bacterial gene carriage (9, 10, 16), coinfecting species (58), and many other factors. In this study, we detail an instance that goes beyond presence or absence of virulence factors, showing that possession of particular allelic variants of a critical adhesin of UPEC modulates the pathogenic process. We have combined an evolutionary analysis of *fimH*, multiple clinical UPEC isolates, representative in vivo models of infection, and biochemical structure–function correlation to explain how the identity of individual amino acid residues, far from the ligand binding "active site" (Fig. 1), alter FimH binding affinity likely through modulation of conformational dynamics, governing virulence of two pathogenic UPEC strains.

Adhesive pili assembled by the chaperone-usher pathway (CUP), such as P and type 1 pili, contain adhesins at their tips that play important roles in host–pathogen interactions. Each sequenced UPEC strain has been found to encode numerous CUP operons (59). Some CUP adhesins are known to recognize specific receptors with stereochemical specificity, such as FimH

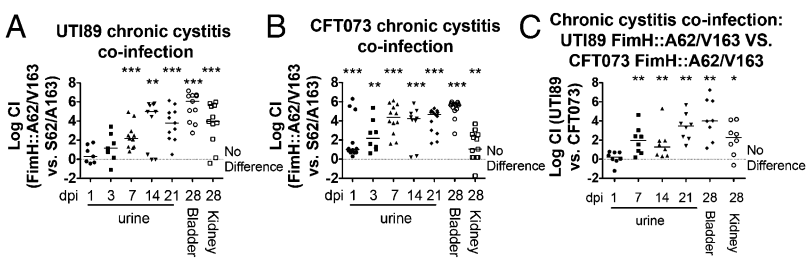

Fig. 4. FimH::A62/V163 displaces FimH::S62/A163 during chronic coinfection. Coinfections were conducted (*A*) between UTI89 with FimH::A62/V163 and FimH::S62/A163, (*B*) between CFT073 with FimH::A62/V163 and FimH::S62/A163, and (*C*) between UTI89 FimH::A62/V163 and CFT073 FimH::A62/V163. Urine was collected at days 1, 3, 7, 14, and 21 d postinfection (dpi), and bladder and kidney titers were determined at 28 dpi. Log_{10} of competitive indices of the mice experiencing chronic cystitis is plotted as determined via plating on selective antibiotics. $n = 2$–3 experiments with 5–10 total mice per group. Wilcoxon signed rank test was conducted to evaluate whether the median value was significantly different from 0; $*p < 0.05$, $**P < 0.01$, $***P < 0.005$.

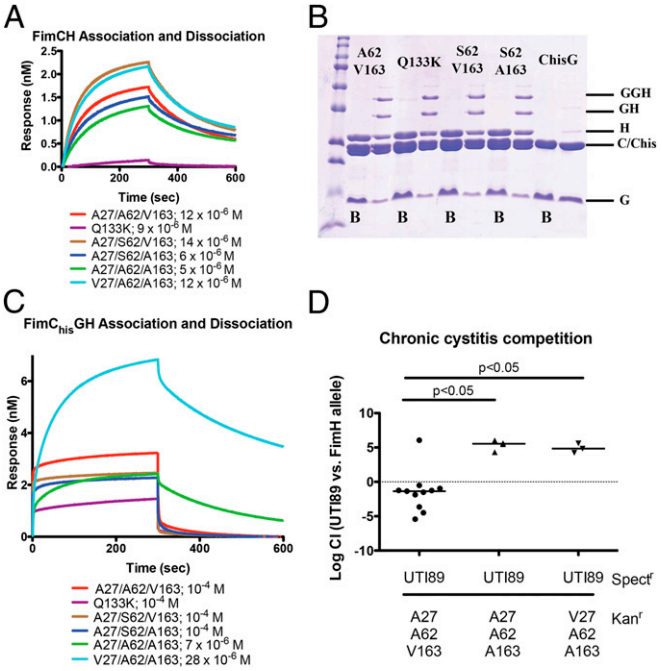

Fig. 5. Effect of FimH on mannose binding and chronic fitness. (*A*) Representative curves showing FimCH association to, and dissociation from, immobilized BSA-mannose at indicated concentrations. Two biological replicates conducted. (*B*) Representative 14% SDS/PAGE gel indicating select variants in $FimC_{His}GH$ samples. "B" marks the boiled lanes. (*C*) Representative curves showing $FimC_{His}GH$ association to, and dissociation from, immobilized BSA-mannose at the indicated concentrations. Representative of three biological replicates with two technical replicates each with combined K_D data shown in Table 2. (*D*) Four-week bladder titer is shown for mice experiencing chronic cystitis with coinfections of the listed strains. n = 1–3 experiments with 5–10 mice each with only chronic cystitis mice displayed.

for mannosylated glycoproteins. Type 1 pili, like other CUP pili, are encoded in a gene cluster comprised of regulatory genes (FimB, FimE), a major pilin subunit (FimA), a periplasmic chaperone (FimC), an outer-membrane usher (FimD), minor tip pilins (FimF, FimG), and the adhesin (FimH). Type 1 pili, like P pili and others, are composite structures, consisting of long, rigid, helical rods made up of FimA, joined at the distal end to a short, linear fiber consisting of FimF, FimG, and the FimH adhesin (60, 61). Tip adhesins consist of two domains: a lectin domain and a pilin domain (Fig. 1). Pilin domains and subunits are incomplete Ig-like folds, encoding just six of the needed seven strands, and thus pilin subunits require the action of dedicated periplasmic chaperones for folding and stability. We discovered that the molecular basis of chaperone-assisted folding was a reaction that we named donor-strand complementation (DSC) (62–64), in which the chaperone transiently completes the Ig-like fold of each subunit, providing the missing seventh beta strand needed for pilin subunit folding (65). The DSC subunit–chaperone complex holds the subunit in a primed high-energy state with connecting loops disordered and the subunit hydrophobic core incompletely collapsed (64–66). These complexes are then differentially targeted to the outer membrane usher (67, 68) (Fig. 6*A*), which is a five-domain gated channel that catalyzes pilus assembly by driving subunit polymerization in a reaction we termed donor strand exchange (DSE). Each of the nonadhesin subunits contains a short N-terminal extension (Nte). DSE occurs in a zip-in–zip-out mechanism where an incoming subunit's Nte zips into the chaperone-bound groove of a nascently incorporated subunit at the growing terminus of the pilus, resulting in chaperone dissociation (69). This process allows the final folding of the subunit with the collapse of the hydrophobic core and the ordering of loop regions, such that every subunit in the pilus completes the Ig fold of its neighbor. The usher converts subunit binding and folding energy into work, acting by sequential allosteric interactions, promoting sequential DSE and incorporation of subunits into the growing pilus while stably maintaining contact with the growing pilus and ensuring the integrity of the outer-membrane barrier in the absence of ATP (70, 71).

FimH has a distal mannose binding lectin domain ($FimH_L$) and a proximal pilin domain ($FimH_p$). The FimG pilin adapts FimH to the tip of the pilus (Fig. 1). Le Trong et al. recently compared $FimH_L$ and Fim tip crystal structures and found that FimH adopts at least two conformations with $FimH_L$, elongated or compact (Figs. 1 and 6*A*) (37, 72). Functional biochemical assays indicated that mannose binds tightly to the elongated $FimH_L$, but weakly, if at all, to the compact $FimH_L$ (37, 46). Recent structural "snapshots" of pilus assembly captured these same FimH conformations during its assembly across the usher: elongated while still bound to FimC before DSE and compact after DSE with FimG, which incorporates FimH into the pilus tip and its extrusion through the usher pore (Fig. 6*A*, *Insets*) (47, 71).

The advent of high-throughput sequencing has allowed the examination of hundreds of *fimH* alleles, providing insight into the evolutionary process of this virulence factor (29, 39). FimH is highly conserved both in clinical and commensal *E. coli* isolates, with all alleles encoding identical amino acids at 90% of the positions (29). The mannose-binding pocket of FimH is invariant among sequenced UPEC, but residues 27, 62, and 163 outside of this binding pocket showed evidence of positive selection (Fig. 1), suggesting that the identity of residues at these positions can confer increased fitness in the urinary tract (29, 39). All of the positively selected residues in FimH are in locations previously identified to displace significantly between elongated and compressed conformations, suggesting that residues may impart steric clashes in one conformation or the other (Fig. 1) (37, 48, 73).

The FimH of the two prototypical UPEC isolates, UTI89 (a cystitis isolate) and CFT073 (a pyelonephritic/sepsis isolate), is identical at residues 27 (both having A), but differs at 62 and 163; UTI89 expresses A62/V163 and CFT073 expresses S62/

Table 2. Affinity values and fits for *fimH* allele complexes

FimH allele*	FimCH mean K_D, μM	Mean fit (R^2)	$FimC_{his}GH$ mean K_D, μM	Mean fit (R^2)	Pathogenesis†	
					Acute	Chronic
Q133K	0	0.46	7193 ± 2957	0.94	–	–
A27/S62/V163	3.6 ± 0.2	0.99	3198 ± 1917	0.99	+	–
A27/S62/A163 (CFT073)	1.5 ± 0.8	0.99	252 ± 110	0.98	+	+
A27/A62/V163 (UTI89)	4.2 ± 0.6	0.99	119 ± 33	0.98	++	++
V27/A62/A163	3.0 ± 0.0	0.99	2.4 ± 0.2	0.98	–	–
A27/A62/A163	1.7 ± 0.0	0.99	7.0 ± 0.6	0.98	?	–

*Relative to UTI89 FimH, where applicable.
†From Figs. 2, 3, and 5*D*, or inferred based on data from ref. 29. Acute and chronic infection describes pathogenesis in single infection or coinfection relative to UTI89 FimH::A27/A62/V163 listed as ++. +, less virulent than UTI89, but still pathogenic; –, defective.

A163. Here, we demonstrate that both of these alleles show high affinity for mannose when complexed with FimC and an intermediate affinity when complexed with FimG in a tip-like $FimC_{his}GH$ complex. Strains harboring a *fimH* sequence coding for A27/A62/V163, present in the cystitis isolates NU14 and UTI89, demonstrated increased fitness in the bladder compared with strains expressing A27/S62/A163, present in UPEC 536 and CFT073, as determined in single infections and coinfections at 4 wk (Table 2, Fig. 6*B*). Because strains with FimH::A27/S62/A163 were essentially absent in 4 wk bladders (Figs. 4 and 6*B*), it is likely that bottlenecks enforced by innate defenses were more easily transcended by strains harboring FimH::A27/A62/V163, likely because of differences in binding and invasion efficiencies (Fig. 6*B*) leading to higher IBC numbers during early infection (18). In addition, the UTI89 *fimH* allele demonstrated enhanced fitness relative to all of the other tested wild-type and mutant variations of these alleles during chronic cystitis (Table 2), when the superficial facet cells are completely denuded (20), suggesting continued selection based on *fimH* allele during chronic infection.

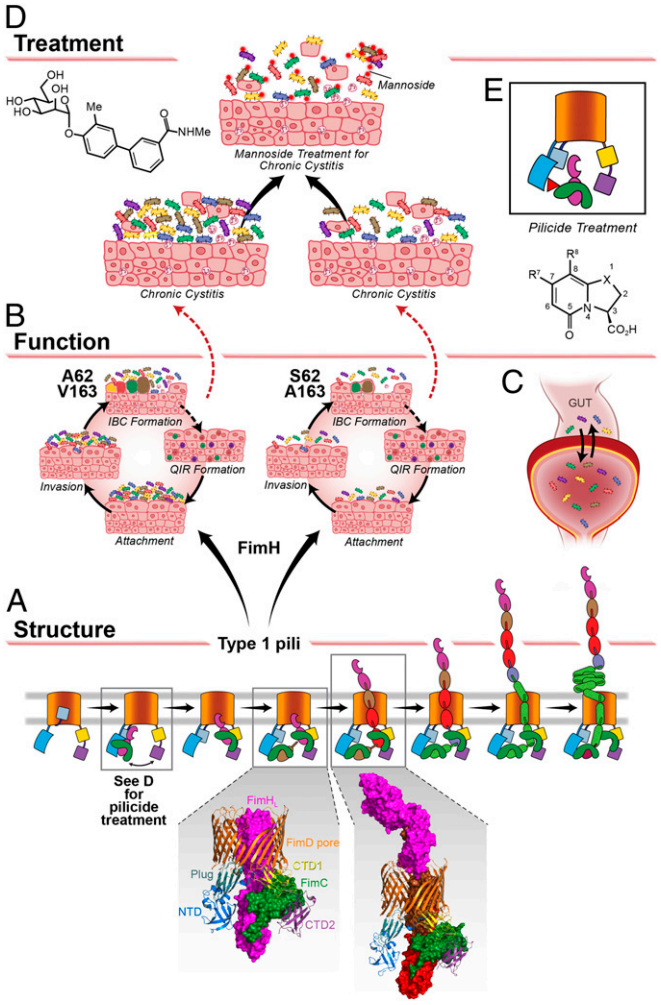

Fig. 6. Structure–function–treatment model of UPEC pathogenesis. (*A*) Model of pilus biogenesis including delivery of chaperone–subunit complexes to the N terminal domain (NTD) (blue) of the usher (orange) with transfer to the C-terminal domain (CTD)s (yellow and fuschia). The next subunit reacts with the previous by DSE polymerizing the pilus rod. *Insets* represent recent crystal structures demonstrating the orientation of FimH as it binds to and exits the usher (47, 71) (PDB ID code: 3RFZ; and PDB ID code: 4J30). (*B*) UPEC pathogenic cascade showing type 1 piliated UPEC attaching to superficial cells of the bladder, invasion into these cells, and replication in the cytoplasm to form IBCs. Mice can then either resolve the infection with potential recurrences thereafter or develop persistent bacteriuria and chronic cystitis. (*C*) The dynamics of transmission from the gut to the bladder and vice versa is an intriguing concept that is just now beginning to be studied (6). (*D*) Mannoside treatment can detach bacteria from the bladder epithelium during chronic cystitis leading to clearance. (*E*) Pilicides block the ability of the pilus to polymerize.

All of the FimH alleles tested, except Q133K, exhibited high affinity for mannose when complexed with FimC and held in the elongated conformation, and all naturally occurring FimH alleles exhibited a low or intermediate affinity for mannose when incorporated into the tip structure. Interestingly, although UTI89 FimH functions with an A62 and CFT073 functions with an A163, in a survey of *fimH* sequences from naturally occurring *E. coli* strains, the combination of A62/A163 has never been observed. We show that A62/A163 variants (both FimH::V27/A62/A163 and FimH::A27/A62/A163) retain their high affinity for mannose even when incorporated into tip-like complexes, suggesting that FimH::A62/A163 does not adopt the low-affinity compact conformation when in the pilus tip or that its transition to the high-affinity elongated form is greatly enhanced in the presence of mannose. Despite their increased relative affinity for mannose, strains harboring these *fimH* alleles were severely attenuated, and it was previously shown that FimH::V27/A62/A163 does not form IBCs at 6 hpi (29). This disparity may reflect a critical role in pathogenesis for the compact state in pathogenesis and/or for the ability to convert between the compact and elongated conformation states. The elongated conformation may prevent detachment from the uroplakin receptor, making UPEC more vulnerable to TLR4-mediated expulsion from the urothelium (74). Alternatively, the compact or low-affinity state may be needed within the IBC or to resist shear stress in the urinary tract. Sokurenko and coworkers discovered that FimH binds via a "catch-bond" mechanism in which shear force can influence the strength of binding (75, 76). We posit that a dynamic equilibrium of FimH between the two conformations may allow UPEC to resist shear forces within host niches and that residues at positions 27, 62, and 163 may impact the transitioning between the two conformations. It is possible that FimH::A62/A163 has dramatically higher mannose binding affinity in its compact state, thus potentiating transitioning to the elongated state, but the binding pocket of the compact state of FimH is partially occluded and would have to adapt to accommodate mannose to an appreciable degree (37).

Possession of an alanine at position 62 (instead of serine) has been associated with increased virulence, mannose binding, and an increased ability to bind to collagen (29, 34, 77). Further, it was previously determined that mutation of position 62 from a serine to a leucine or glutamic acid enhanced bacterial binding to surface mannose (73), consistent with our findings. Our work would suggest that mutation of this residue from alanine to serine, in the context of V163 (FimH::A27/S62/V163) may decrease the ability of FimH to transition from the compressed, low-affinity conformation seen in the tip in the absence of mannose to the high-affinity, elongated conformation. Thus, the combination of amino acids present at positions 62 and 163 modulates FimH function. We propose that evolutionary pressure on UPEC isolates has led to the selection of FimH residue combinations, which alter the stability or affinity of one conformation or the other, affecting the equilibrium between the different conformations and thus mannose affinity and pathogenesis. The FimH complexes with intermediate binding affinity, A27/A62/V163 and A27/S62/A163, expressed by UTI89 and CFT073, respectively, may be able to dynamically switch between conformations, allowing them to bind to and invade superficial facet cells, and then detach and enter the cytoplasm to replicate into IBCs (Figs. 5 and 6*B*).

We have recently characterized the population dynamics between gastrointestinal (GI) and bladder niches in women suffering UTI (Fig. 6*C*). At the time of UTI in four patients, we found that the UPEC strain that occupied the urinary tract was the same as the dominant *E. coli* found in the GI tract (6). Interestingly, in one patient from this study, when a recurrent UTI was caused by a different strain of UPEC, this new strain also replaced the previous strain in the GI tract, implying that

increased fitness in the urinary tract was not accompanied by a decrease in fitness in the gut, which was corroborated by a fitness analysis in both niches in animal models (Fig. 6*C*) (6). The most common combination of positively selected residues that we found in both healthy human feces as well as the urinary tracts of women suffering UTI was A27/S62/V163, perhaps suggesting a generalist FimH, capable of colonizing both niches. The low affinity for mannose of a UTI89 FimH mutated to carry this combination of residues suggests that this FimH allele likely is very poor in adopting an elongated conformation, perhaps signifying that the compact conformation is of greater importance throughout infection. Additionally, residues elsewhere in FimH may further modulate the conformation equilibrium. The two combinations that we found only in diseased urine but not in healthy feces (FimH::A27/A62/V163 and FimH::A27/S62/A163) suggest that these alleles may have increased virulence in the urinary tract. It is possible that *E. coli* expressing this allele may invariably lead to UTI, which may accelerate the decision to seek treatment. Selection for *fimH* is likely quite different in the urinary and GI tracts due to differences in shear stress, which has been shown to influence FimH binding, due to urine flow and peristalsis (75, 76, 78). Thus, it will be interesting to assess the effect of FimH variants in the GI tract. These types of studies and investigations similar to those performed by Chen et al. in which multiple niches are sampled longitudinally may further help refine the source–sink hypothesis of virulence and pathoadaptation of UPEC in multiple niches (6, 79).

Increasing rates of antibiotic resistance in bacteria, including uropathogens (80), the spread of multidrug-resistant strains (49), and the dearth of new antibiotic candidates in pharmaceutical development pipelines make a compelling argument and opportunity for novel virulence-based therapeutics (Fig. 6 *D* and *E*) (81). Multiple groups are investigating methods to inhibit the ability of UPEC to bind and invade bladder tissue as well as to block catheter colonization via antiadhesive small-molecule inhibitors and vaccines (Fig. 6 *D* and *E*) (82–85). High-affinity mannosides that bind in the FimH binding pocket have been shown to block invasion and IBC formation as well as biofilm formation on abiotic surfaces (82, 83). Additionally, mannosides delivered orally were shown to dramatically reduce bacterial burden during chronic cystitis (Fig. 6*D*) (83). Pilicides have been designed, aimed at disrupting assembly of multiple CUP pili to incapacitate bacterial adhesion in various tissue niches and body habitats (Fig. 6*E*) (86). These molecules work, in part, by blocking the interaction of the usher with chaperone–subunit complexes, thus blocking pilus assembly (86). These antivirulence therapeutics hold promise for targeting recalcitrant UPEC infections.

Conclusion

Our current understanding of the pathogenic lifestyles of UPEC is in part an extension of the molecular and structural characterization of type 1 pili. This development has led to a new understanding of clinical UTIs and its complicating factors. Through genomic and pathoadaption studies, we have elucidated a connection between evolutionary pressures, protein structural dynamics, and disease pathogenesis. UTIs are one of the greatest contributors to antibiotic consumption and thus an important driver of the development of antibiotic resistance. In addition to the therapeutic strategies addressed above, therapeutics that block the interconversion of the FimH adhesin or that lock it in either conformation would impede UPEC pathogenesis (73, 87). Analyses of other pathogens and virulence genes by combining positive selection analyses, in vivo models of pathogenesis, and biochemical and structural characterization could lead to identification of similar targets for the development of novel therapeutics that will be needed to fend off the looming crisis of multidrug-resistant bacterial pathogens.

Materials and Methods

Bacterial Strains. UTI89 strains with chromosomally integrated *fimH* variants were generated using the λ Red recombinase system (88) and are the same as previously published (29). The same method was used to create similar *fimH* variants in CFT073. Creation of HK-marked antibiotic-resistant strains was conducted similarly.

Mouse Infections. Infections, LacZ staining of bladders, and ex vivo gentamicin protection assays were conducted as previously described (18, 45, 89). All mouse infection studies were approved by the Animal Studies Committee of Washington University School of Medicine, St. Louis, MO.

Protein Purification and Biolayer Interferometry. OCTET was used to attain biolayer interferometry (BLI) progress curves from purified protein complexes, which allowed us to extract kinetic parameters (k_{on}, k_{dis}, and K_D). See *SI Materials and Methods* for more details. Analysis was conducted on ForteBio Data Analysis 6.4. Processed data were fit globally for each variant at three concentrations between 1.25 and 12 μM for FimCH and 1.8–200 μM for $FimC_{his}GH$ per experiment in a 1:1 kinetic binding model.

Statistical Analysis. Statistical analysis was performed in GraphPad Prism 5.0. The cfu values of zero were set to the limit of detection of the assay. Competitive Index (CI) = (cfu_{output} strain A/cfu_{output} strain B)/(cfu_{input} strain A/cfu_{input} strain B). Wilcoxon Signed Rank was used on log transformed CI to determine whether the median value was different from 0. Statistical analysis to compare median values between groups was determined by Mann–Whitney *U* test. To compare proportions of mice experiencing persistent bacteriuria and chronic cystitis, we used Fisher's Exact Test. $P < 0.05$ was considered significant.

ACKNOWLEDGMENTS. We thank members of the S.J.H. laboratory for helpful suggestions. We also thank Will Planer for help with strain creation, Dan Liu for urine collection, Patrick Olson for technical assistance with mouse infections, and Wandy Beatty for TEM studies. Thanks to Stanley Falkow, Staffan Normark, Tom Silhavy, Carl Frieden, and Jeffrey Gordon for guidance and inspiration to S.J.H. throughout his career. S.J.H. was supported by National Institutes of Health (NIH) National Institute of Allergy and Infectious Diseases (NIAID) Grant R01 AI029549, NIAID Grant R01 AI048689, Office of Research on Women's Health (ORWH)/National Institute of Diabetes and Digestive and Kidney Diseases (NIDDK) Grant P50 DK064540, NIDDK Grant R01 DK051406, NIAID Grant U01 AI095542, and NIAID Grant R01 AI099099. D.J.S. was supported by NIH NIDDK Grant F30 DK096751, and S.L.C. was supported by NIDDK K01 DK081620 and an administrative supplement.

1. Foxman B, Brown P (2003) Epidemiology of urinary tract infections: Transmission and risk factors, incidence, and costs. *Infect Dis Clin North Am* 17(2):227–241.
2. Mabeck CE (1972) Treatment of uncomplicated urinary tract infection in non-pregnant women. *Postgrad Med J* 48(556):69–75.
3. Scholes D, et al. (2000) Risk factors for recurrent urinary tract infection in young women. *J Infect Dis* 182(4):1177–1182.
4. Mysorekar IU, Hultgren SJ (2006) Mechanisms of uropathogenic Escherichia coli persistence and eradication from the urinary tract. *Proc Natl Acad Sci USA* 103(38): 14170–14175.
5. Schilling JD, Lorenz RG, Hultgren SJ (2002) Effect of trimethoprim-sulfamethoxazole on recurrent bacteriuria and bacterial persistence in mice infected with uropathogenic Escherichia coli. *Infect Immun* 70(12):7042–7049.
6. Chen SL, et al. (2013) Genomic diversity and fitness of E. coli strains recovered from the intestinal and urinary tracts of women with recurrent urinary tract infection. *Sci Transl Med* 5(184):184ra160.
7. Johnson JR, Stamm WE (1989) Urinary tract infections in women: Diagnosis and treatment. *Ann Intern Med* 111(11):906–917.
8. Gupta K, Hooton TM, Stamm WE (2001) Increasing antimicrobial resistance and the management of uncomplicated community-acquired urinary tract infections. *Ann Intern Med* 135(1):41–50.
9. Norinder BS, Köves B, Yadav M, Brauner A, Svanborg C (2012) Do Escherichia coli strains causing acute cystitis have a distinct virulence repertoire? *Microb Pathog* 52(1):10–16.
10. Vejborg RM, Hancock V, Schembri MA, Klemm P (2011) Comparative genomics of Escherichia coli strains causing urinary tract infections. *Appl Environ Microbiol* 77(10): 3268–3278.
11. Connell I, et al. (1996) Type 1 fimbrial expression enhances Escherichia coli virulence for the urinary tract. *Proc Natl Acad Sci USA* 93(18):9827–9832.
12. Mulvey MA, Schilling JD, Hultgren SJ (2001) Establishment of a persistent Escherichia coli reservoir during the acute phase of a bladder infection. *Infect Immun* 69(7): 4572–4579.
13. Wu XR, Sun TT, Medina JJ (1996) In vitro binding of type 1-fimbriated Escherichia coli to uroplakins Ia and Ib: Relation to urinary tract infections. *Proc Natl Acad Sci USA* 93(18):9630–9635.
14. Mulvey MA, et al. (1998) Induction and evasion of host defenses by type 1-piliated uropathogenic Escherichia coli. *Science* 282(5393):1494–1497.
15. Anderson GG, et al. (2003) Intracellular bacterial biofilm-like pods in urinary tract infections. *Science* 301(5629):105–107.
16. Garofalo CK, et al. (2007) Escherichia coli from urine of female patients with urinary tract infections is competent for intracellular bacterial community formation. *Infect Immun* 75(1):52–60.

17. Rosen DA, Hooton TM, Stamm WE, Humphrey PA, Hultgren SJ (2007) Detection of intracellular bacterial communities in human urinary tract infection. *PLoS Med* 4(12):e329.
18. Schwartz DJ, Chen SL, Hultgren SJ, Seed PC (2011) Population dynamics and niche distribution of uropathogenic Escherichia coli during acute and chronic urinary tract infection. *Infect Immun* 79(10):4250–4259.
19. Walters MS, et al. (2011) Kinetics of uropathogenic Escherichia coli metapopulation movement during urinary tract infection. *mBio* 3(1):e00303–e00311.
20. Hannan TJ, Mysorekar IU, Hung CS, Isaacson-Schmid ML, Hultgren SJ (2010) Early severe inflammatory responses to uropathogenic E. coli predispose to chronic and recurrent urinary tract infection. *PLoS Pathog* 6(8):e1001042.
21. Hannan TJ, et al. (2012) Host-pathogen checkpoints and population bottlenecks in persistent and intracellular uropathogenic Escherichia coli bladder infection. *FEMS Microbiol Rev* 36(3):616–648.
22. Schwartz DJ, Hultgren SJ (2012) Uropathogenic *Escherichia coli* virulence and gene regulation. *Regulation of bacterial virulence*, eds Vasil ML, Darwin AJ (ASM Press, Washington, D.C.), pp 135–155.
23. Chan CY, St John AL, Abraham SN (2013) Mast cell interleukin-10 drives localized tolerance in chronic bladder infection. *Immunity* 38(2):349–359.
24. Hull RA, Gill RE, Hsu P, Minshew BH, Falkow S (1981) Construction and expression of recombinant plasmids encoding type 1 or D-mannose-resistant pili from a urinary tract infection Escherichia coli isolate. *Infect Immun* 33(3):933–938.
25. Brinton CC, Jr. (1959) Non-flagellar appendages of bacteria. *Nature* 183(4664): 782–786.
26. Hung C-S, et al. (2002) Structural basis of tropism of Escherichia coli to the bladder during urinary tract infection. *Mol Microbiol* 44(4):903–915.
27. Le Trong I, et al. (2010) Donor strand exchange and conformational changes during E. coli fimbrial formation. *J Struct Biol* 172(3):380–388.
28. Hanson MS, Brinton CC, Jr. (1988) Identification and characterization of *E. coli* type-1 pilus tip adhesion protein. *Nature* 332(6161):265–268.
29. Chen SL, et al. (2009) Positive selection identifies an in vivo role for FimH during urinary tract infection in addition to mannose binding. *Proc Natl Acad Sci USA* 106(52):22439–22444.
30. Sokurenko EV, et al. (1998) Pathogenic adaptation of Escherichia coli by natural variation of the FimH adhesin. *Proc Natl Acad Sci USA* 95(15):8922–8926.
31. Weissman SJ, et al. (2007) Differential stability and trade-off effects of pathoadaptive mutations in the Escherichia coli FimH adhesin. *Infect Immun* 75(7):3548–3555.
32. Klein EA, Gitai Z (2013) Draft genome sequence of uropathogenic Escherichia coli strain J96. *Genome Announc* 1(1):e00245-12.
33. Brzuszkiewicz E, et al. (2006) How to become a uropathogen: Comparative genomic analysis of extraintestinal pathogenic Escherichia coli strains. *Proc Natl Acad Sci USA* 103(34):12879–12884.
34. Johnson JR, et al. (2001) Clonal and pathotypic analysis of archetypal Escherichia coli cystitis isolate NU14. *J Infect Dis* 184(12):1556–1565.
35. Hochhut B, et al. (2006) Role of pathogenicity island-associated integrases in the genome plasticity of uropathogenic Escherichia coli strain 536. *Mol Microbiol* 61(3): 584–595.
36. Blattner FR, et al. (1997) The complete genome sequence of Escherichia coli K-12. *Science* 277(5331):1453–1462.
37. Le Trong I, et al. (2010) Structural basis for mechanical force regulation of the adhesin FimH via finger trap-like beta sheet twisting. *Cell* 141(4):645–655.
38. Chen SL, et al. (2006) Identification of genes subject to positive selection in uropathogenic strains of Escherichia coli: A comparative genomics approach. *Proc Natl Acad Sci USA* 103(15):5977–5982.
39. Weissman SJ, et al. (2006) Clonal analysis reveals high rate of structural mutations in fimbrial adhesins of extraintestinal pathogenic Escherichia coli. *Mol Microbiol* 59(3): 975–988.
40. Ochman H, Selander RK (1984) Standard reference strains of Escherichia coli from natural populations. *J Bacteriol* 157(2):690–693.
41. Hooton TM, et al. (1996) A prospective study of risk factors for symptomatic urinary tract infection in young women. *N Engl J Med* 335(7):468–474.
42. Czaja CA, et al. (2009) Prospective cohort study of microbial and inflammatory events immediately preceding Escherichia coli recurrent urinary tract infection in women. *J Infect Dis* 200(4):528–536.
43. Marschall J, et al. (2012) Both host and pathogen factors predispose to Escherichia coli urinary-source bacteremia in hospitalized patients. *Clin Infect Dis* 54(12):1692–1698.
44. Mobley HL, et al. (1990) Pyelonephritogenic Escherichia coli and killing of cultured human renal proximal tubular epithelial cells: role of hemolysin in some strains. *Infect Immun* 58(5):1281–1289.
45. Hung C-S, Dodson KW, Hultgren SJ (2009) A murine model of urinary tract infection. *Nat Protoc* 4(8):1230–1243.
46. Bouckaert J, et al. (2006) The affinity of the Fimh fimbrial adhesin is receptor-driven and quasi-independent of Escherichia coli pathotypes. *Mol Microbiol* 61(6):1556–1568.
47. Geibel S, Procko E, Hultgren SJ, Baker D, Waksman G (2013) Structural and energetic basis of folded-protein transport by the FimD usher. *Nature* 496(7444):243–246.
48. Choudhury D, et al. (1999) X-ray structure of the FimC-FimH chaperone-adhesin complex from uropathogenic Escherichia coli. *Science* 285(5430):1061–1066.
49. Totsika M, et al. (2011) Insights into a multidrug resistant Escherichia coli pathogen of the globally disseminated ST131 lineage: Genome analysis and virulence mechanisms. *PLoS ONE* 6(10):e26578.
50. Hooper LV, Littman DR, Macpherson AJ (2012) Interactions between the microbiota and the immune system. *Science* 336(6086):1268–1273.
51. Dethlefsen L, Relman DA (2011) Incomplete recovery and individualized responses of the human distal gut microbiota to repeated antibiotic perturbation. *Proc Natl Acad Sci USA* 108(Suppl 1):4554–4561.
52. Koch R (1884) An address on cholera and its bacillus. *BMJ* 2(1236):453–459.
53. Falkow S (1988) Molecular Koch's postulates applied to microbial pathogenicity. *Rev Infect Dis* 10(Suppl 2):S274–S276.
54. Hawn TR, et al. (2009) Toll-like receptor polymorphisms and susceptibility to urinary tract infections in adult women. *PLoS ONE* 4(6):e5990.
55. Ragnarsdóttir B, et al. (2010) Toll-like receptor 4 promoter polymorphisms: Common TLR4 variants may protect against severe urinary tract infection. *PLoS ONE* 5(5): e10734.
56. Ikäheimo R, et al. (1996) Recurrence of urinary tract infection in a primary care setting: Analysis of a 1-year follow-up of 179 women. *Clin Infect Dis* 22(1):91–99.
57. Hooton TM (2001) Recurrent urinary tract infection in women. *Int J Antimicrob Agents* 17(4):259–268.
58. Kline KA, Schwartz DJ, Gilbert NM, Hultgren SJ, Lewis AL (2012) Immune modulation by group B Streptococcus influences host susceptibility to urinary tract infection by uropathogenic Escherichia coli. *Infect Immun* 80(12):4186–4194.
59. Spurbeck RR, et al. (2011) Fimbrial profiles predict virulence of uropathogenic Escherichia coli strains: Contribution of ygi and yad fimbriae. *Infect Immun* 79(12): 4753–4763.
60. Kuehn MJ, Heuser J, Normark S, Hultgren SJ (1992) P pili in uropathogenic E. coli are composite fibres with distinct fibrillar adhesive tips. *Nature* 356(6366):252–255.
61. Jones CH, et al. (1995) FimH adhesin of type 1 pili is assembled into a fibrillar tip structure in the Enterobacteriaceae. *Proc Natl Acad Sci USA* 92(6):2081–2085.
62. Holmgren A, Bränden CI (1989) Crystal structure of chaperone protein PapD reveals an immunoglobulin fold. *Nature* 342(6247):248–251.
63. Kuehn MJ, et al. (1993) Structural basis of pilus subunit recognition by the PapD chaperone. *Science* 262(5137):1234–1241.
64. Sauer FG, Pinkner JS, Waksman G, Hultgren SJ (2002) Chaperone priming of pilus subunits facilitates a topological transition that drives fiber formation. *Cell* 111(4): 543–551.
65. Sauer FG, et al. (1999) Structural basis of chaperone function and pilus biogenesis. *Science* 285(5430):1058–1061.
66. Verger D, Bullitt E, Hultgren SJ, Waksman G (2007) Crystal structure of the P pilus rod subunit PapA. *PLoS Pathog* 3(5):e73.
67. Dodson KW, Jacob-Dubuisson F, Striker RT, Hultgren SJ (1993) Outer-membrane PapC molecular usher discriminately recognizes periplasmic chaperone-pilus subunit complexes. *Proc Natl Acad Sci USA* 90(8):3670–3674.
68. Saulino ET, Thanassi DG, Pinkner JS, Hultgren SJ (1998) Ramifications of kinetic partitioning on usher-mediated pilus biogenesis. *EMBO J* 17(8):2177–2185.
69. Soto GE, et al. (1998) Periplasmic chaperone recognition motif of subunits mediates quaternary interactions in the pilus. *EMBO J* 17(21):6155–6167.
70. Volkan E, et al. (2012) Domain activities of PapC usher reveal the mechanism of action of an Escherichia coli molecular machine. *Proc Natl Acad Sci USA* 109(24):9563–9568.
71. Phan G, et al. (2011) Crystal structure of the FimD usher bound to its cognate FimC-FimH substrate. *Nature* 474(7349):49–53.
72. Bouckaert J, et al. (2005) Receptor binding studies disclose a novel class of high-affinity inhibitors of the Escherichia coli FimH adhesin. *Mol Microbiol* 55(2):441–455.
73. Rodriguez VB, et al. (2013) Allosteric coupling in the bacterial adhesive protein FimH. *J Biol Chem* 288(33):24128–24139.
74. Bishop BL, et al. (2007) Cyclic AMP-regulated exocytosis of Escherichia coli from infected bladder epithelial cells. *Nat Med* 13(5):625–630.
75. Yakovenko O, et al. (2008) FimH forms catch bonds that are enhanced by mechanical force due to allosteric regulation. *J Biol Chem* 283(17):11596–11605.
76. Aprikian P, et al. (2011) The bacterial fimbrial tip acts as a mechanical force sensor. *PLoS Biol* 9(5):e1000617.
77. Pouttu R, et al. (1999) Amino acid residue Ala-62 in the FimH fimbrial adhesin is critical for the adhesiveness of meningitis-associated Escherichia coli to collagens. *Mol Microbiol* 31(6):1747–1757.
78. Dreux N, et al. (2013) Point mutations in FimH adhesin of Crohn's disease-associated adherent-invasive Escherichia coli enhance intestinal inflammatory response. *PLoS Pathog* 9(1):e1003141.
79. Sokurenko EV, Gomulkiewicz R, Dykhuizen DE (2006) Source-sink dynamics of virulence evolution. *Nat Rev Microbiol* 4(7):548–555.
80. Zhanel GG, et al.; NAUTICA Group (2006) Antibiotic resistance in Escherichia coli outpatient urinary isolates: Final results from the North American Urinary Tract Infection Collaborative Alliance (NAUTICA). *Int J Antimicrob Agents* 27(6):468–475.
81. Cusumano CK, Hultgren SJ (2009) Bacterial adhesion—a source of alternate antibiotic targets. *IDrugs* 12(11):699–705.
82. Schwardt O, et al. (2011) Design, synthesis and biological evaluation of mannosyl triazoles as FimH antagonists. *Bioorg Med Chem* 19(21):6454–6473.
83. Cusumano CK, et al. (2011) Treatment and prevention of urinary tract infection with orally active FimH inhibitors. *Sci Transl Med* 3(109):109ra115.
84. Langermann S, et al. (1997) Prevention of mucosal Escherichia coli infection by FimH-adhesin-based systemic vaccination. *Science* 276(5312):607–611.
85. Guiton PS, et al. (2012) Combinatorial small-molecule therapy prevents uropathogenic Escherichia coli catheter-associated urinary tract infections in mice. *Antimicrob Agents Chemother* 56(9):4738–4745.
86. Pinkner JS, et al. (2006) Rationally designed small compounds inhibit pilus biogenesis in uropathogenic bacteria. *Proc Natl Acad Sci USA* 103(47):17897–17902.
87. Tchesnokova V, et al. (2011) Type 1 fimbrial adhesin FimH elicits an immune response that enhances cell adhesion of Escherichia coli. *Infect Immun* 79(10):3895–3904.
88. Datsenko KA, Wanner BL (2000) One-step inactivation of chromosomal genes in Escherichia coli K-12 using PCR products. *Proc Natl Acad Sci USA* 97(12):6640–6645.
89. Justice SS, Lauer SR, Hultgren SJ, Hunstad DA (2006) Maturation of intracellular Escherichia coli communities requires SurA. *Infect Immun* 74(8):4793–4800.